

Emergent criticality and universality class of spin and charge density wave transitions of two-component lattice Bose gases in optical cavities at finite temperature

Liang He*

*Guangdong Provincial Key Laboratory of Quantum Engineering and Quantum Materials,
SPTE, South China Normal University, Guangzhou 510006, China*

Su Yi†

*CAS Key Laboratory of Theoretical Physics, Institute of Theoretical Physics,
Chinese Academy of Sciences, Beijing 100190, China and
School of Physical Sciences & CAS Center for Excellence in Topological Quantum Computation,
University of Chinese Academy of Sciences, Beijing 100049, China*

We investigate the finite temperature spin density wave (SDW) and charge density wave (CDW) transition of two-component lattice spinor Bose gases in optical lattices in the Mott-insulator limit. At the temperature scale around half of the on-site interaction energy, we find a new critical regime emerges and features, in particular, a new bicritical line and two critical lines associated with the finite temperature SDW-CDW, homogeneous-SDW, and homogeneous-CDW transition, respectively. Direct calculation of the critical exponents for the scaling behavior and investigating on the effective theory in this critical regime show that they belong to the five-dimensional Ising universality class, clearly manifesting the long-range character of the system's interaction. Our prediction of the emergent criticality can be readily observed by current experimental setups operated at the intermediate temperature scale around half the on-site interaction energy.

Many-body systems with high microscopic symmetry can give rise to the rich interplay between various macroscopic orders. Well-known examples in the context of conventional condensed matter physics, range from the multicritical points associated with various magnetic orders found in antiferromagnets with weak lattice anisotropy [1, 2], over the multiferroics where the magnetic order and the electric order are coupled in a non-trivial way holding the potential in greatly improving the energy efficiency of electronic devices [3], to the even more elusive scenario in high-temperature superconductors where the charge density wave (CDW), spin density wave (SDW), and superconducting order can compete, intertwine, or even form the “vestigial order” in certain cases [4]. Noticing, however, interactions in these conventional condensed matter systems are all short-ranged, while in the context of ultracold atom physics, not only short-range interacting, but also long-range interacting quantum many-body systems can be realized and well-controlled in experiments. This thus provides an ideal platform for investigating the rich interplay between various macroscopic orders in the presence of long-range interactions.

Among various long-range interacting ultracold atom systems, Bose gases in optical cavities are unique in the sense that they assume *infinite-long range* (ILR) interactions. In particular, ultracold Bose gases with internal spin degrees of freedom have recently been realized in experiments [5–11], featuring both an ILR spin-spin and an ILR density-density interaction mediated by cavity photons. In the experiments of Ref. [5, 9], two macroscopic orders, namely the SDW and the CDW order, have been observed and a first-order transition between

these two ordered phases have been identified by tuning the ratio between these two types of ILR interactions. Noticing current experiments have mainly focused on the low-temperature regime where the temperature is much smaller than all other energy scales in the system, it is intriguing to expect that at a comparable temperature scale, a new scenario for the interplay between the two macroscopic orders could emerge. This thus gives rise to the fundamental question of the existence and the universality class of the possible new criticality that is absent in the low-temperature regime, in particular, the multicritical behavior associated with the interplay between the SDW and the CDW order.

In this paper, we address this question for two-component lattice Bose gases in optical cavities. To this end, we establish the finite-temperature phase diagram of the system in the deep Mott-insulator limit (cf. Fig. 1) and investigate the emergent critical scaling of the system (cf. Fig. 2). More specifically, we find the following. (i) An emergent critical regime featuring in particular a new bicritical line associated with the SDW-CDW transition at finite temperature. At low temperatures, we find transitions between each two of the three phases, namely, the homogeneous, the SDW, and the CDW phase are all first-order transitions, where the SDW (CDW) order parameter assumes finite jump $\Delta\bar{\chi}$ ($\Delta\bar{\phi}$) when the transition boundary is crossed [cf. Fig. 1(b)]. When the temperature increases, $\Delta\bar{\chi}$ and $\Delta\bar{\phi}$ for the homogeneous-SDW and the homogeneous-CDW transitions decrease, finally vanish at their respective critical points, and both transitions become second-order transitions [cf. Fig. 1(c) and Figs. 2(c, d)]. At the same time, a new bicritical point emerges, where the first-order SDW-CDW transi-

tion terminates at this point with vanishing order parameter jumps $\Delta\bar{\chi}$ and $\Delta\bar{\phi}$ [cf. Fig. 1(d) and Figs. 2(a, b)]. (ii) The universality class of the emergent critical scaling belongs to the five-dimensional (5D) Ising universality class (cf. Fig. 2). This clearly shows that the criticality of the system is strongly influenced by and thus bear the long-range characteristic of its interactions.

System and model in the deep Mott-insulator limit.— Among current diverse experimental setups of multi-component Bose gases in optical cavities [5–11], here we concentrate on the experimental setups in Ref. [5, 9], where, in particular, cavity mediated spin-spin interactions were realized. Moreover, an additional static square optical lattice is assumed in the system, similar to what has been realized for single-component Bose gases in optical cavities [12]. For this type of two-component lattice spinor Bose gases in optical cavities, their physics in a large parameter regime can be described by an ILR interacting Hubbard-type Hamiltonian, which consists of a conventional hopping part and an interaction part (see Supplemental Material [13] for the derivation of the lattice model). Here, we focus on the physics in the deep Mott-insulator limit which is completely determined by the interaction part of the Hamiltonian whose explicit form reads

$$\hat{H} = \frac{1}{2} \sum_{i,\sigma\sigma'} U_{\sigma\sigma'} \hat{n}_{i,\sigma} (\hat{n}_{i,\sigma'} - \delta_{\sigma\sigma'}) - \frac{1}{L} \left[U_D (\hat{N}_e - \hat{N}_o)^2 + U_S (\hat{S}_e - \hat{S}_o)^2 \right]. \quad (1)$$

The first term of the Hamiltonian (1) describes the on-site intra- and inter-component interactions whose strengths are characterized by $U_{\sigma\sigma'}$ with $\sigma(\sigma') = \pm$ being the component index. The second term in Eq. (1) describes the cavity-mediated ILR density-density and spin-spin interactions with their strengths characterized by U_D and U_S , respectively. Noticing in this term, both U_D and U_S are further rescaled by the total number of lattice sites L according to the Kac prescription [14] in order to restore the conventional thermodynamical limit. Here, the two interpenetrating square sub-lattices of the complete square lattice are referred to as “even” (e) and “odd” (o) lattice, respectively. $\hat{n}_{i,\sigma}$ is the particle number operator that counts the number of atoms with component index σ at site i . $\hat{N}_{e(o)} \equiv \sum_{i \in e(o)} (\hat{n}_{i,+} + \hat{n}_{i,-})$ and $\hat{S}_{e(o)} \equiv \sum_{i \in e(o)} (\hat{n}_{i,+} - \hat{n}_{i,-})$ are the total density and total spin operator of the even (odd) sub-lattice.

From the Hamiltonian (1) we notice that the system assumes both a \mathbb{Z}_2 -symmetry with respect to the two sub-lattices, i.e., exchanging the sub-lattice indices “ e ” and “ o ”, and a \mathbb{Z}_2 -symmetry with respect to the two-components, i.e., exchanging the component indices “ $-$ ” and “ $+$ ”. The ILR density-density interaction favors a CDW phase that breaks the \mathbb{Z}_2 -symmetry between the two sub-lattices, while the ILR spin-spin interaction fa-

vors an SDW phase that breaks both \mathbb{Z}_2 -symmetries. The competition among these two types of ILR interaction and the short-range on-site interaction gives rise to phase transitions among the SDW, CDW, and the homogeneous phase as observed in experiments focusing at fixed low temperatures [5]. At the temperature scale that is comparable with the energy scales of interactions, one would expect that thermal fluctuations could give rise to new physics that is absent in the low-temperature regime. Indeed, as we shall see in the following, new criticality associated to phase transitions among the SDW, CDW, and the homogeneous phase arises in this finite temperature regime.

Finite-temperature phase diagram and emergent criticality at intermediate temperature scale.— To establish the complete finite-temperature phase diagram, we directly calculate the quantum grand partition function $Z = \text{tr}[e^{-\beta(\hat{H} - \mu_\sigma \sum_i \hat{n}_{i,\sigma})}]$ of the system, which can be formulated as an integral with respect to the SDW order parameter field χ and the CDW order parameter field ϕ [13], and explicitly reads

$$Z = \frac{\beta L}{\pi} \sqrt{U_D U_S} \iint_{-\infty}^{+\infty} d\chi d\phi e^{-\beta L \Omega_{\{U_S, U_D, U_{\sigma\sigma'}, \mu_\sigma, \beta\}}(\phi, \chi)}, \quad (2)$$

with

$$\begin{aligned} & \Omega_{\{U_S, U_D, U_{\sigma\sigma'}, \mu_\sigma, \beta\}}(\phi, \chi) \\ & \equiv -\frac{1}{2\beta} \sum_{\eta=\pm 1} \ln \left[\sum_{n_\pm=0}^{+\infty} e^{-\beta \left(\sum_{\sigma\sigma'} \frac{1}{2} U_{\sigma\sigma'} n_\sigma (n_\sigma - \delta_{\sigma\sigma'}) - \sum_\sigma \mu_\sigma n_\sigma \right)} \right. \\ & \quad \left. e^{-2\beta\eta[U_D \phi(n_+ + n_-) + U_S \chi(n_+ - n_-)]} \right] + U_D \phi^2 + U_S \chi^2. \end{aligned} \quad (3)$$

Here, μ_σ is the chemical potential for the species with component index σ , and $\beta = (k_B T)^{-1}$ with k_B being the Boltzmann constant and T being the temperature. Order parameter fields χ and ϕ in Eq. (2) are introduced via the standard Hubbard-Stratonovich transformation, and their expectation values $\bar{\chi}$ and $\bar{\phi}$ correspond exactly to the CDW and SDW order parameter, respectively, i.e., $\bar{\chi} \equiv \langle \chi \rangle = \langle \hat{S}_e - \hat{S}_o \rangle / L$, $\bar{\phi} \equiv \langle \phi \rangle = \langle \hat{N}_e - \hat{N}_o \rangle / L$. In the thermodynamic limit $L \rightarrow \infty$, the partition function Z is exactly determined by its saddle point integration, hence SDW and CDW order parameters $\bar{\phi}$ and $\bar{\chi}$ are determined by the value of (ϕ, χ) that minimizes $\Omega_{\{U_S, U_D, U_{\sigma\sigma'}, \mu_\sigma, \beta\}}(\phi, \chi)$ (see Supplemental Material [13] for more technical details). The summation in Eq. (3) can be numerically evaluated at sufficiently high accuracy with a large enough cut-off on n_σ . This enables us to map out the complete finite-temperature phase diagram as we shall now discuss.

In the following, we focus on the balanced case with unit filling for both species of atoms, i.e., $\langle \sum_i \hat{n}_{i,\sigma} \rangle / L = 1$

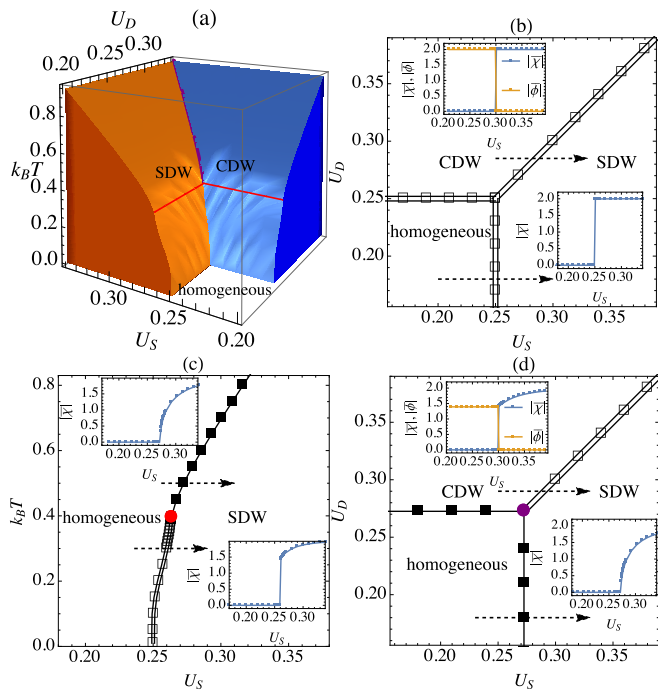


FIG. 1. (a) Finite temperature phase diagram of the system at the balanced unit filling for both species of atoms, i.e., $\langle \sum_i \hat{n}_{i,\sigma} \rangle / L = 1$. $U_{+-} \ll U_{++} = U_{--}$ is assumed, and $U_{\sigma\sigma}$ is set to be the energy unit. The SDW and CDW phase regions are highlighted by orange and blue, respectively. Two critical lines (marked by the thick red lines) emerge at the temperature $k_B T = 0.395$. The left (right) critical line separates the first-order homogeneous-SDW (CDW) transition from the second-order homogeneous-SDW (CDW) transition. Above these two critical lines, both the homogeneous-SDW and the homogeneous-CDW transition are second-order transitions, and their transition boundaries (second-order critical surfaces) meet at a bicritical line (marked by the thick purple line). (b) Phase diagram at the fixed temperature with $k_B T = 0.1$. The transitions between each two of the homogeneous, CDW and SDW phase are all first-order transitions whose boundaries are marked by double solid curves and open squares. Insets: The order parameter dependence on U_S when the first-order CDW-SDW (homogeneous-SDW) transition boundary is crossed. (c) Phase diagram at the fixed $U_D = 0.2$. At low temperatures, the homogeneous-SDW transition is a first-order transition, whose boundary is marked by open squares and a double solid curve. It becomes a second-order transition (marked by filled squares and a solid curve) at and above a critical point (marked by the red dot) whose temperature $T_{CP} = 0.395/k_B$. Insets: The upper (lower) inset shows the SDW order parameter dependence on U_S with $k_B T = 0.3$ ($k_B T = 0.5$), clearly showing the transition is a first-order (second-order) transition for $T < T_{CP}$ ($T > T_{CP}$). (d) Phase diagram at the fixed temperature with $k_B T = 0.5$. The SDW-CDW transition still keeps as a first-order transition, whose boundary is marked by a double solid curve and open squares, while it terminates at a bicritical point (marked by the purple dot), where the two second-order transition boundaries meet (marked by solid curves and solid squares). Insets: The order parameter dependence on U_S when the first-order CDW-SDW (the second-order homogeneous-SDW) transition boundary is crossed. See text for more details.

for $\sigma = \pm$. In addition, the intra-component interaction strengths U_{++} and U_{--} are assumed to be equal and much larger than the inter-component interaction strength U_{+-} , i.e., $U_{+-} \ll U_{++} = U_{--}$. This corresponds to the case where the physics associated with the internal “spin” degrees of freedom is dominated by the IIR spin-spin interaction. For the convenience of the discussion, the on-site inter-component interaction $U_{\sigma\sigma}$ is set to be the energy unit in the following. The finite-temperature phase diagram of the system for this case is shown in Fig. 1(a), which consists of three phase regions that correspond to the SDW, the CDW, and the homogeneous phase, respectively. At low temperature, the transitions between each two of these three phases are all first-order transitions as shown in Fig. 1(b), which is a cross-section of the phase diagram Fig. 1(a) at $k_B T = 0.1$. This corroborates recent findings in experiments [11].

In the parameter regime where the temperature scale is comparable to the on-site interaction energy [cf. the vicinal region of the two red lines and the purple line in Fig. 1(a)], rich critical behavior appear. This manifests particularly in the emergence of the two critical lines and the bicritical line [marked by red and purple, respectively, in Fig. 1(a)].

The two critical lines consist of critical points at which the first-order homogeneous-SDW transition or the homogeneous-CDW transition terminates and changes to the second-order transition. For instance, in Fig. 1(c), a cross-section of the phase diagram Fig. 1(a) at $U_D = 0.2$ is shown, and one can directly observe that the homogeneous-SDW transition changes from a first-order transition to a second-order one at the critical point with $T_{CP} = 0.39/k_B$ (marked by the red dot in the plot). In fact, the second-order homogeneous-SDW and homogeneous-CDW transitions above these two critical lines give rise to a critical line consisting of a new type of critical point that is absent in the corresponding single-component systems, namely, the bicritical point [cf. the purple dot in Fig. 1(d)].

The emergence of the bicritical points can be straightforwardly seen by monitoring the change of the $U_S - U_D$ phase diagram of the system when the temperature is increased, as illustrated by Fig. 1(b) and Fig. 1(d) which show two typical $U_S - U_D$ phase diagrams at relatively low ($k_B T = 0.1$) and high ($k_B T = 0.5$) temperature. We can directly see from these two diagrams that at low temperatures all the transition boundaries are first-order ones, while in the temperature regime above the two-critical lines, both the homogeneous-SDW and homogeneous-CDW transition boundary become the second-order transition boundary [cf. the two solid lines in Fig. 1(d)] and change the point where these two boundaries meet to a bicritical point [cf. the purple dot in Fig. 1(d)], at which the first-order SDW-CDW transition boundary also terminates.

The emergence of these two critical lines and the bi-

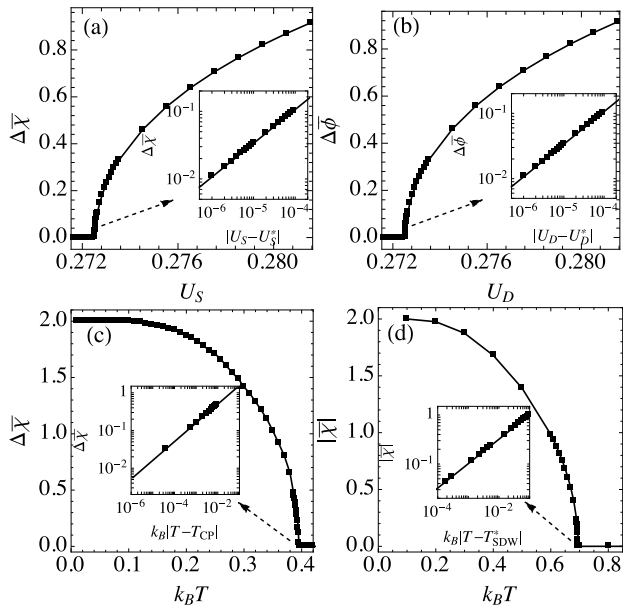


FIG. 2. Critical scaling behavior of the SDW and CDW order parameter in the critical regime. (a, b) Scaling behavior of order parameter jumps $\Delta\bar{\chi}$ and $\Delta\bar{\phi}$ in the vicinity of the bicritical point with $k_B T = 0.5$. The main plots show the interaction strength dependence of $\Delta\bar{\chi}$ and $\Delta\bar{\phi}$ along the first-order SDW-CDW transition boundary [cf. Fig. 1(d)]. The insets show the power law fits to the interaction strength dependence of $\Delta\bar{\phi}$ and $\Delta\bar{\chi}$ in the vicinity of the bicritical point $(U_D^*, U_S^*) = (0.2725, 0.2725)$, clearly manifesting the power law scaling behavior $\Delta\bar{\chi} \propto |U_S - U_S^*|^{0.499}$ and $\Delta\bar{\phi} \propto |U_D - U_D^*|^{0.499}$. (c) SDW order parameter jump $\Delta\bar{\chi}$ versus temperature along the first-order transition boundary shown in Fig. 1(c), showing a power law scaling $\Delta\bar{\chi} \propto |T - T_{CP}|^{0.497}$ near the critical point $k_B T_{CP} = 0.395$ as shown by the inset in the plot. (d) Temperature dependence of SDW order parameter $|\bar{\chi}|$ with (U_S, U_D) kept fixed at $(0.3, 0.2)$ when T is tuned across a second-order homogeneous-SDW transition point with $k_B T_{SDW}^* = 0.69525$, showing a power law scaling of $\propto (T - T_{SDW}^*)^{0.496}$ near the second-order transition as shown by the inset in the plot. See text for more details.

critical line gives rise to a new critical regime that is absent at low temperatures where all the transitions are first-order ones. As we shall see in the following, in this critical regime, the system manifests critical power law scalings characteristic of its long-range interactions.

Critical scaling and universality class of transitions among SDW, CDW, and homogeneous phases at finite temperatures.—For the SDW-CDW transition, irrespective of the temperature, it is always a first-order transition, i.e., both the SDW and CDW order parameter show finite jump when either U_S or U_D is tuned across the first-order SDW-CDW transition boundary [cf. Fig. 1(b, d)]. Consequentially, neither ϕ nor χ shows any critical power law scaling. However, in the temperature regime where the bicritical point emerges, the SDW-CDW transition can indeed assume a type of critical scaling in the vicin-

ity of the bicritical point, manifesting in both order parameter jumps, namely, $\Delta\bar{\chi}$ and $\Delta\bar{\phi}$. As we can see from Figs. 2(a, b), which show the ILR interaction strength dependence of $\Delta\bar{\chi}$ and $\Delta\bar{\phi}$ along a first-order SDW-CDW transition boundary that terminates at a bicritical point [cf. Fig. 1(d)], both $\Delta\bar{\chi}$ and $\Delta\bar{\phi}$ decrease monotonously with respect to the IRL interaction strengths and finally vanish at the bicritical point. Power law fits to the interaction strength dependence of $\Delta\bar{\chi}$ and $\Delta\bar{\phi}$ in the vicinity of the bicritical point $(U_D^*, U_S^*) = (0.2725, 0.2725)$ [cf. the purple dot in Fig. 1(d)] as shown in the insets of Figs. 2(a, b), clearly show the power law critical scaling behavior $\Delta\bar{\chi} \propto |U_S - U_S^*|^{0.499}$ and $\Delta\bar{\phi} \propto |U_D - U_D^*|^{0.499}$.

For the homogeneous-SDW and the homogeneous-CDW transition, there are two types of critical scaling behavior associated with each of them. The first type manifests in the order parameter jump in the vicinity of the critical point where the first-order transition change to a second-order one [cf. Fig. 1(c)]. Let us take the homogeneous-SDW transition for instance. As we can see from Fig. 2(c), which shows the temperature dependence of $\Delta\bar{\chi}$ along a first-order homogeneous-SDW transition boundary that terminates at a critical point [cf. Fig. 1(c)], $\Delta\bar{\chi}$ decrease monotonously with respect to temperature and finally vanish at the critical point. Power law fit to the temperature dependence of $\Delta\bar{\chi}$ in the vicinity of the critical point $k_B T_{CP} = 0.395$ [cf. the red dot in Fig. 1(c)] as shown in the inset of Fig. 2(c) clearly shows the power law critical scaling behavior $\Delta\bar{\chi} \propto |T - T_{CP}|^{0.497}$. The second type of critical scaling behavior manifests in the order parameter in the vicinity of the second-order transition. Let us still take the homogeneous-SDW transition for instance. As we can see from Fig. 2(d), which shows the temperature dependence of $|\bar{\chi}|$ when (U_S, U_D) is kept fixed at $(0.3, 0.2)$, and T is tuned across a second-order homogeneous-SDW transition point with $k_B T_{SDW}^* = 0.69525$ [cf. Fig. 1(c)], $|\bar{\chi}|$ decrease monotonously with respect to the temperature and finally vanish at the transition point. Power law fit to the temperature dependence of $|\bar{\chi}|$ in the vicinity of the second-order transition point as shown in the inset of Fig. 2(d) clearly shows the power law critical scaling behavior $|\bar{\chi}| \propto |T - T_{SDW}^*|^{0.496}$.

Interestingly, one can notice that the power law scaling behavior for different transitions manifest almost the same critical exponent with the value $1/2$. This strongly suggests they should originate from the same effective critical theory. Indeed, as we shall see below, all these scaling behavior can be well-described by an effective Ginzburg-Landau (GL) theory with a double \mathbb{Z}_2 symmetry.

In the critical regime, both the CDW and the SDW order parameters are small enough to allow a systematic expansion of the system's free energy F with respect to them. The double \mathbb{Z}_2 symmetry of the system determine the allowed terms in the expansion, whose explicit form

reads

$$F = -\frac{1}{2}r_\phi\bar{\phi}^2 - \frac{1}{2}r_\chi\bar{\chi}^2 + \frac{1}{4}u_\phi\bar{\phi}^4 + \frac{1}{4}u_\chi\bar{\chi}^4 + \frac{1}{2}u_{\phi\chi}\bar{\phi}^2\bar{\chi}^2, \quad (4)$$

with r_ϕ , r_χ , u_ϕ , u_χ , and $u_{\phi\chi}$ being the GL coefficients. Comparing to the single-component case, the novel aspect of physics, in this case, is the competition between the two ordered phases, namely, the CDW and the SDW phase, that is driven by the relative strength between U_D and U_S . In the spirit of Ginzburg-Landau effective theory, to describe this scenario, we assume that $r_\phi \propto (U_D - U_D^*)$ and $r_\chi \propto (U_S - U_S^*)$ with (U_D^*, U_S^*) being the critical point around which both order parameters, i.e., $\bar{\phi}$ and $\bar{\chi}$, are small. u_ϕ , u_χ , and $u_{\phi\chi}$ are positive fixed GL parameters that do not depend on the tuning parameter U_D and U_S . By analyzing the saddle points of F (see Supplemental Material [13] for analysis details), depending on the sign of $u_{\phi\chi}^2 - u_\phi u_\chi$, one can find two distinct phase diagrams for the effective theory (4) as shown in Fig. 3. Comparing to results from direct calculations as shown in Fig. 1(d), one naturally expects the system under consideration is described by the GL theory with $u_\phi u_\chi < u_{\phi\chi}^2$, where there is a direct first-order transition between the SDW and CDW phases. Direct calculations within the GL theory with $u_\phi u_\chi < u_{\phi\chi}^2$ show that the order parameter jumps $\Delta\bar{\phi}$ and $\Delta\bar{\chi}$ along the first-order SDW-CDW transition line assumes the forms $\Delta\bar{\phi} = \sqrt{r_\phi/u_\phi}$ and $\Delta\bar{\chi} = \sqrt{r_\chi/u_\chi}$ [13]. Noticing r_ϕ and r_χ depend linearly on interaction strengths, one thus directly obtains the following scaling law

$$\Delta\bar{\chi} \propto |U_S - U_S^*|^{1/2}, \quad \Delta\bar{\phi} \propto |U_D - U_D^*|^{1/2}. \quad (5)$$

We remark here that from the phase diagrams of the effective theory (4), the tetracritical point is in principle allowed by the GL theory with the double \mathbb{Z}_2 symmetry. Interestingly, in the experimental setup with two-component Bose gases in the presence of two optical resonators [6], this tetracritical point is indeed observed. This indicates, for the type of experimental systems in Ref. [6], its GL effective theory is the one with $u_\phi u_\chi > u_{\phi\chi}^2$. To discuss the scaling behavior associated with the homogeneous-SDW transition or the homogeneous-CDW transition, since either CDW or the SDW order is identically zero in the transition under consideration, the effective theory (4) in fact degenerates to the one with the single \mathbb{Z}_2 symmetry and can be straightforwardly analyzed as what has been done in the single-component case [15]. Take the homogeneous-SDW transition, for instance, this analysis results in power law scaling $\Delta\bar{\chi} \propto |T - T_{\text{CP}}|^{1/2}$ in the vicinity of the critical point, and $|\bar{\chi}| \propto |T - T_{\text{SDW}}^*|^{1/2}$ in the vicinity of the second-order transition. In fact, from the structure of the phase diagram Fig. 3(a), it is straightforward to see that the scaling behavior for $\Delta\bar{\chi}$ ($\Delta\bar{\phi}$) with respect to the

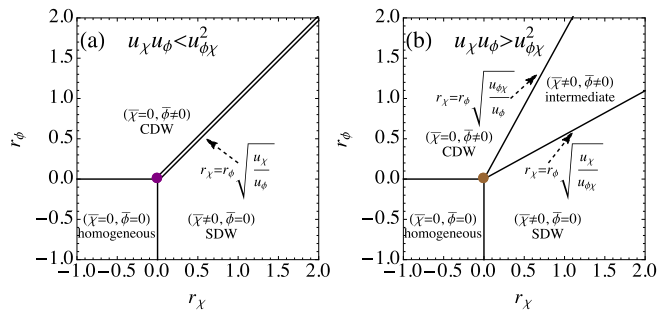


FIG. 3. Phase diagram of the effective GL theory (4) with double \mathbb{Z}_2 symmetry that shows either a bicritical point or a tetracritical point, depending on the sign of $u_{\phi\chi}^2 - u_\phi u_\chi$. Solid curves stand for the second-order transition boundaries, while the double solid ones stand for the first-order transition boundaries. Left panel: For $u_{\phi\chi}^2 > u_\phi u_\chi$, the phase diagram support a bicritical point (marked by the purple dot) at $(r_\phi = 0, r_\chi = 0)$ where two second-order phase transition boundaries meet. Right panel: For $u_{\phi\chi}^2 < u_\phi u_\chi$, the phase diagram support a tetracritical point (marked by the brown dot) at $(r_\phi = 0, r_\chi = 0)$ where four second-order phase transition boundaries meet. See text for more details.

interaction strength U_S (U_D) in Eq. (5) is the same as the one for $\bar{\chi}$ ($\bar{\phi}$) of the second-order homogeneous-SDW (homogeneous-CDW) transition, which is determined by the effective GL theories with the single \mathbb{Z}_2 symmetry. Therefore, all the scaling exponents discussed above is governed essentially by the same effective GL theories with the single \mathbb{Z}_2 symmetry.

By comparing the critical exponents from the GL effective theory and the ones from direct calculations, one immediately notices remarkable agreement that seems counter-intuitive at first sight, since long-range fluctuations are omitted in the effective GL theory, and it is only expected to provide rough estimations of the critical exponents for the 2D system under consideration. In fact, this good agreements between the mean-field type effective GL theory and direct exact calculations, originate from the fact that long-range fluctuations in the critical regime are strongly suppressed by the ILR interactions in the system, hence making effective GL theory a precise theory in the critical regime. Such a similar promotion of an effective GL theory to a precise effective critical theory is also identified in the single-component Bose gases in optical cavities [15]. Noticing the corresponding critical exponent of the 5D Ising model is exactly 1/2 [16] and can be obtained by the same effective GL theory, this thus concludes that the emergent criticality of the system at finite temperature belongs to the 5D Ising universality class, manifests clearly the long-range character of its interactions.

Conclusions.—Thermal fluctuations at intermediate temperature regime can strongly influence the competition between magnetic and density order of multi-component Bose gases in optical cavities, giving rise to

rich critical behavior: The first-order SDW-homogeneous and CDW-homogeneous transition become second-order transitions, and at the same time giving rise to a new bicritical line, where the first-order SDW-CDW transition terminates at this line with vanishing order parameter jumps. The critical scaling behavior in this critical regime belong to the five-dimensional Ising universality class, clearly characterizing the long-range nature of the system's interactions. With current well-established experimental techniques for detecting the SDW and CDW order [5, 12], we expect our findings can be directly observed by current experimental setups [5] operated at the temperature scale around half of the on-site energy. We believe our work will stimulate further experimental and also theoretical investigations on possible emergent critical behavior in multicomponent Bose gases in optical cavities in the presence of thermal fluctuations, particularly beyond the deep Mott-insulator limit.

This work was supported by NSFC (Grant No. 11874017, No. 11674334, and No. 11947302), GDSTC under Grant No. 2018A030313853, Science and Technology Program of Guangzhou (Grant No. 2019050001), and START grant of South China Normal University.

* liang.he@scnu.edu.cn

† syi@itp.ac.cn

- [1] Y. Shapira and S. Foner, *Phys. Rev.* **1**, 3083 (1970).
- [2] H. Rohrer and Ch. Gerber, *Phys. Rev. Lett.* **38**, 909 (1977).
- [3] N. A. Spaldin, S. W. Cheong, and R. Ramesh, *Phys. Today* **10**, 38 (2010).
- [4] E. Fradkin, S. A. Kivelson, and J. M. Tranquada, *Rev. Mod. Phys.* **87**, 457 (2015).
- [5] M. Landini, N. Dogra, K. Kroeger, L. Hruby, T. Donner, and T. Esslinger, *Phys. Rev. Lett.* **120**, 223602 (2018).
- [6] A. Morales, P. Zupancic, J. Léonard, T. Esslinger, and T. Donner, *Nature Materials* **17**, 686 (2018).
- [7] R. M. Kroeze, Y. Guo, V. D. Vaidya, J. Keeling, and B. L. Lev, *Phys. Rev. Lett.* **121**, 163601 (2018).
- [8] A. Morales, D. Dreon, X. Li, A. Baumgärtner, P. Zupancic, T. Donner, and T. Esslinger, *Phys. Rev. A* **100**, 013816 (2019).
- [9] N. Dogra, M. Landini, K. Kroeger, L. Hruby, T. Donner, and T. Esslinger, *Science* **366**, 1496 (2019).
- [10] E. J. Davis, G. Bentsen, L. Homeier, T. Li, and M. H. Schleier-Smith, *Phys. Rev. Lett.* **122**, 010405 (2019).
- [11] X. Li, D. Dreon, P. Zupancic, A. Baumgärtner, A. Morales, W. Zheng, N. R. Cooper, T. Donner, and T. Esslinger, arXiv:2004.08398.
- [12] R. Landig, L. Hruby, N. Dogra, M. Landini, R. Mottl, T. Donner, and T. Esslinger, *Nature (London)* **532**, 476 (2016).
- [13] See Supplemental Material for discussions on relevant technical details.
- [14] M. Kac, G. E. Uhlenbeck, and P. C. Hemmer, *J. Math. Phys.* **4**, 216 (1963).
- [15] L. He and S. Yi, arXiv:2002.08861.
- [16] M. Aizenman, *Phys. Rev. Lett.* **47**, 1 (1981).

Supplementary Material for “Emergent criticality and universality class of spin and charge density wave transitions of two-component lattice Bose gases in optical cavities at finite temperature”

Liang He*

*Guangdong Provincial Key Laboratory of Quantum Engineering and Quantum Materials,
SPTE, South China Normal University, Guangzhou 510006, China*

Su Yi†

*CAS Key Laboratory of Theoretical Physics, Institute of Theoretical Physics,
Chinese Academy of Sciences, Beijing 100190, China and
School of Physical Sciences & CAS Center for Excellence in Topological Quantum Computation,
University of Chinese Academy of Sciences, Beijing 100049, China*

HAMILTONIAN OF TWO-COMPONENT LATTICE BOSE GASES IN OPTICAL CAVITIES

In current experiments, multicomponent Bose gases are loaded in the free space inside cavities. We consider here a closely related system where a two-component Bose gas is loaded in a two dimensional (2D) square optical lattice within an optical cavity. As we shall present in the following, the Hamiltonian of this system can be derived from the atom-photon interacting model that corresponds to the experimental setup in Ref. [1].

Our starting point is the single-particle atom-photon interacting model for two-component or pseudo-spin 1/2 bosonic atoms in a 2D square optical lattice which reads

$$\begin{aligned} \hat{H}_{\text{sp}} = & \left\{ \frac{|\hat{\mathbf{p}}|^2}{2m} + V_{2D}[\cos^2(k\hat{x}) + \cos^2(k\hat{z})] \right\} \otimes \mathbb{I} \\ & + \lambda_D(\hat{a}^\dagger + \hat{a}) \cos(k\hat{x}) \cos(k\hat{z}) \otimes \mathbb{I} \\ & - i\lambda_S(\hat{a}^\dagger - \hat{a}) \cos(k\hat{x}) \cos(k\hat{z}) \otimes \sigma_z \\ & - \Delta_c \hat{a}^\dagger \hat{a} + U_0 \hat{a}^\dagger \hat{a} \cos^2(k\hat{x}) \otimes \mathbb{I} \end{aligned} \quad (\text{S-1})$$

where λ_D (λ_S) is the spin-independent (spin-dependent) atom-photon interaction strength, V_{2D} is the strength of the 2D optical lattice potential, \hat{a}^\dagger (\hat{a}) is the creation (annihilation) operator for the photons in the cavity, Δ_c is the detuning between the frequency of the cavity photon and the frequency of the z -lattice beam, U_0 is the maximum light shift per atom, \mathbb{I} is the 2×2 identity matrix, and σ_z is the conventional Pauli matrix. After taking the lowest band approximation, we can directly write down the corresponding many-body atom-photon Hamiltonian

in the complete second quantization form, namely

$$\begin{aligned} \hat{H}_{\text{AP}} & \quad \quad \quad (\text{S-2}) \\ = & \int d\mathbf{r} \hat{\Psi}^\dagger(\mathbf{r}) \left[-\frac{\hbar\nabla^2}{2m} + V_{2D}(\cos^2(kx) + \cos^2(kz)) \right] \hat{\Psi}(\mathbf{r}) \\ & + \int d\mathbf{r} \hat{\Psi}^\dagger(\mathbf{r}) [\lambda_D(\hat{a}^\dagger + \hat{a}) \cos(kx) \cos(kz)] \hat{\Psi}(\mathbf{r}) \\ & + \int d\mathbf{r} \hat{\Psi}^\dagger(\mathbf{r}) [-i\lambda_S(\hat{a}^\dagger - \hat{a}) \cos(kx) \cos(kz)] \sigma_z \hat{\Psi}(\mathbf{r}) \\ & + \left(\int d\mathbf{r} \hat{\Psi}^\dagger(\mathbf{r}) U_0 \cos^2(kx) \hat{\Psi}(\mathbf{r}) - \Delta_c \right) \hat{a}^\dagger \hat{a} \end{aligned}$$

where $\hat{\Psi}(\mathbf{r}) \equiv \left(\sum_{\mathbf{i}} W_{\mathbf{i}}(x, z) \hat{b}_{\mathbf{i},+}, \sum_{\mathbf{i}} W_{\mathbf{i}}(x, z) \hat{b}_{\mathbf{i},-} \right)^T$ with $W_{\mathbf{i}}(x, z)$ being the Wannier function on the site \mathbf{i} in the lowest band and $\hat{b}_{\mathbf{i},\pm}$ being its corresponding annihilation operator for the atom with component index $\sigma = \pm$. After further taking into account the contact interaction between atoms, the system can be well described by the following many-body Hamiltonian

$$\begin{aligned} \hat{H}_{\text{AP}} & \quad \quad \quad (\text{S-3}) \\ = & \frac{1}{2} \sum_{\mathbf{i}, \sigma\sigma'} U_{\sigma\sigma'} \hat{n}_{\mathbf{i},\sigma} (\hat{n}_{\mathbf{i},\sigma'} - \delta_{\sigma\sigma'}) - t \sum_{\langle \mathbf{i}, \mathbf{j} \rangle, \sigma} \left(\hat{b}_{\mathbf{i},\sigma}^\dagger \hat{b}_{\mathbf{j},\sigma} + \text{H.c.} \right) \\ & + \lambda_D(\hat{a}^\dagger + \hat{a}) \left(\hat{N}_e - \hat{N}_o \right) - i\lambda_S(\hat{a}^\dagger - \hat{a}) \left(\hat{S}_e - \hat{S}_o \right) \\ & - (\Delta_c - \delta) \hat{a}^\dagger \hat{a} \end{aligned}$$

where $U_{\sigma\sigma'}$ is the contact interaction strength between atoms with component index σ and σ' , t is the hopping amplitude, and δ is a dispersive shift [2]. Here, $\hat{N}_{e(o)} = \sum_{\mathbf{i} \in e(o)} (\hat{n}_{\mathbf{i},+} + \hat{n}_{\mathbf{i},-})$ and $\hat{S}_{e(o)} = \sum_{\mathbf{i} \in e(o)} (\hat{n}_{\mathbf{i},+} - \hat{n}_{\mathbf{i},-})$, with $\hat{n}_{\mathbf{i},\sigma} \equiv \hat{b}_{\mathbf{i},\sigma}^\dagger \hat{b}_{\mathbf{i},\sigma}$.

To derive the effective Hamiltonian for the atoms only, we first write down the Heisenberg equation of motion for cavity photons with a finite decay rate κ , i.e., $i d\hat{a}/dt = [\hat{a}, \hat{H}_{\text{AP}}] - i\kappa\hat{a}$, whose explicit form reads

$$\begin{aligned} i \frac{d\hat{a}}{dt} = & -(\Delta_c - \delta) \hat{a} - i\kappa \hat{a} \quad \quad \quad (\text{S-4}) \\ & + \lambda_D \left(\hat{N}_e - \hat{N}_o \right) - i\lambda_S \left(\hat{S}_e - \hat{S}_o \right). \end{aligned}$$

Typically, κ is much larger than the atomic recoil energy scale, thus we can approximate \hat{a} as

$$\hat{a} = \frac{\lambda_D (\hat{N}_e - \hat{N}_o) - i\lambda_S (\hat{S}_e - \hat{S}_o)}{\Delta_c - \delta + i\kappa}. \quad (\text{S-5})$$

Plugging the above expression into Eq. (S-3), we thus eliminate the cavity field adiabatically and obtain the effective Hubbard-type Hamiltonian \hat{H}_{Hub} for the atoms only, i.e.,

$$\begin{aligned} \hat{H}_{\text{Hub}} = & -t \sum_{\langle \mathbf{i}, \mathbf{j} \rangle, \sigma} \left(\hat{b}_{\mathbf{i}, \sigma}^\dagger \hat{b}_{\mathbf{j}, \sigma} + \text{H.c.} \right) \\ & + \frac{1}{2} \sum_{\mathbf{i}, \sigma \sigma'} U_{\sigma \sigma'} \hat{n}_{\mathbf{i}, \sigma} (\hat{n}_{\mathbf{i}, \sigma'} - \delta_{\sigma \sigma'}) \\ & - \frac{1}{L} \left[U_{l,D} (\hat{N}_e - \hat{N}_o)^2 + U_{l,S} (\hat{S}_e - \hat{S}_o)^2 \right], \end{aligned} \quad (\text{S-6})$$

with

$$U_{l,D} \equiv -2L\lambda_D^2 \frac{\Delta_c - \delta}{(\Delta_c - \delta)^2 + \kappa^2}, \quad (\text{S-7})$$

$$U_{l,S} \equiv -2L\lambda_S^2 \frac{\Delta_c - \delta}{(\Delta_c - \delta)^2 + \kappa^2}. \quad (\text{S-8})$$

PARTITION FUNCTION AFTER THE HUBBARD-STRONOVICH TRANSFORMATION

The grand quantum partition function for the system in the Mott-insulator limit reads

$$\begin{aligned} Z = & \text{tr} \left[e^{-\beta(\hat{H} - \mu_\sigma \hat{N}_\sigma)} \right] \\ = & \sum_{\{n_{i,\sigma}\}} e^{-\beta(\sum_{i,\sigma,\sigma'} \frac{1}{2} U_{\sigma\sigma'} (n_{i,\sigma} - \delta_{\sigma\sigma'}))} \\ & \times e^{-\beta(-L^{-1}[U_D(N_e - N_o)^2 + U_S(S_e - S_o)^2])}, \end{aligned} \quad (\text{S-9})$$

where $N_{e(o)} = \sum_{i \in e(o)} (n_{i,+} + n_{i,-})$ and $S_{e(o)} = \sum_{i \in e(o)} (n_{i,+} - n_{i,-})$, with $n_{i,\sigma}$ being the eigenvalue of the particle number operator $\hat{n}_{i,\sigma}$. To treat the long-range density-density and spin-spin interaction term, we introduce two Hubbard-Stratonovich transformations in the density and spin channel, respectively, i.e.,

$$\left(\sqrt{\frac{\beta U_D L}{\pi}} \right)^{-1} \exp \left(\beta \frac{U_D}{L} [N_e - N_o]^2 \right) \quad (\text{S-10})$$

$$= \int_{-\infty}^{+\infty} d\phi \exp \left(-\beta U_D \{ L\phi^2 + 2[N_e - N_o]\phi \} \right),$$

$$\left(\sqrt{\frac{\beta U_S L}{\pi}} \right)^{-1} \exp \left(\beta \frac{U_S}{L} [S_e - S_o]^2 \right) \quad (\text{S-11})$$

$$= \int_{-\infty}^{+\infty} d\chi \exp \left(-\beta U_S \{ L\chi^2 + 2[S_e - S_o]\chi \} \right).$$

Plugging the above transformations into the partition function, we arrive at

$$Z = \frac{\beta L}{\pi} \sqrt{U_D U_S} \iint_{-\infty}^{+\infty} d\chi d\phi e^{-\beta L \Omega_{\{U_S, U_D, U_{\sigma\sigma'}, \mu_\sigma, \beta\}}(\phi, \chi)}, \quad (\text{S-12})$$

where

$$\begin{aligned} & \Omega_{\{U_S, U_D, U_{\sigma\sigma'}, \mu_\sigma, \beta\}}(\phi, \chi) \\ & \equiv -\frac{1}{2\beta} \sum_{\eta=\pm 1} \ln \left[\sum_{n_\pm=0}^{+\infty} e^{-\beta \left(\sum_{\sigma\sigma'} \frac{1}{2} U_{\sigma\sigma'} n_\sigma (n_\sigma - \delta_{\sigma\sigma'}) - \sum_\sigma \mu_\sigma n_\sigma \right)} \right. \\ & \quad \left. e^{-2\beta \eta [U_D \phi (n_+ + n_-) + U_S \chi (n_+ - n_-)]} \right] + U_D \phi^2 + U_S \chi^2. \end{aligned} \quad (\text{S-13})$$

Here χ and ϕ assume the physical meaning of the fluctuating SDW and CDW order parameter field, respectively. Their expectation values $\bar{\chi} \equiv \langle \chi \rangle$ and $\bar{\phi} \equiv \langle \phi \rangle$ equal to the SDW and CDW order parameter, respectively, i.e., $\bar{\chi} = \langle \hat{S}_e - \hat{S}_o \rangle / L$, $\bar{\phi} = \langle \hat{N}_e - \hat{N}_o \rangle / L$.

ANALYSIS OF THE GINZBURG-LANDAU EFFECTIVE THEORY WITH A DOUBLE- Z_2 SYMMETRY

Since both the CDW order parameter $\bar{\phi}$ and the SDW order parameter $\bar{\chi}$ are small in the critical regime, one can perform a systematic expansion of the system's free energy with respect to these two order parameters. Up to the fourth order in the order parameters, the double- Z_2 symmetry allowed form of the Ginzburg-Landau (GL) free energy F reads

$$F = -\frac{1}{2} r_\phi \bar{\phi}^2 - \frac{1}{2} r_\chi \bar{\chi}^2 + \frac{1}{4} u_\phi \bar{\phi}^4 + \frac{1}{4} u_\chi \bar{\chi}^4 + \frac{1}{2} u_{\phi\chi} \bar{\phi}^2 \bar{\chi}^2. \quad (\text{S-14})$$

Now let us discuss the interaction-induced transition between the CDW and SDW phase at a fixed temperature that is above the critical temperature which separates the first-order homogeneous-SDW (homogeneous-CDW) transition from the second-order homogeneous-SDW (homogeneous-CDW) transition. In the spirit of Ginzburg-Landau effective theory, we assume that $r_\phi \propto (U_D - U_D^*)$ and $r_\chi \propto (U_S - U_S^*)$ with (U_D^*, U_S^*) being the critical point around which both order parameters, i.e., $\bar{\phi}$ and $\bar{\chi}$, are small. u_ϕ , u_χ , and $u_{\phi\chi}$ are positive fixed GL parameters that do not depend on the tuning parameter U_D and U_S . The saddle point of GL free energy is determined by the equations $\partial F / \partial \bar{\phi} = 0$ and $\partial F / \partial \bar{\chi} = 0$, whose explicit form reads

$$\bar{\phi} (-r_\phi + u_\phi \bar{\phi}^2 + u_{\phi\chi} \bar{\chi}^2) = 0, \quad (\text{S-15})$$

$$\bar{\chi} (-r_\chi + u_\chi \bar{\chi}^2 + u_{\phi\chi} \bar{\phi}^2) = 0. \quad (\text{S-16})$$

By straightforwardly investigating the solution of the above saddle point equations, one can directly find the

phase diagram of the GL effective theory (S-14) can assume two distinct structures depending on the sign of $u_{\phi\chi}^2 - u_\phi u_\chi$.

In the case with $u_{\phi\chi}^2 - u_\phi u_\chi > 0$, the phase diagram assumes two second-order phase transition boundaries that correspond to the homogeneous-SDW and homogeneous-CDW transition and one first-order transition boundary that corresponds to the SDW-CDW transition. The phase with both orders does not exist. These two second-order phase transition boundaries meet at a bicritical point ($r_\phi = 0, r_\chi = 0$) at which the order parameter jumps associated with the first-order SDW-CDW transition vanish, i.e., the first-order SDW-CDW transition boundary terminates at this point. The order parameter jumps assume the forms $\Delta\bar{\phi} = \sqrt{\frac{r_\phi}{u_\phi}}$ and $\Delta\bar{\chi} = \sqrt{\frac{r_\chi}{u_\chi}}$, from which one can conclude the corresponding power law scaling $\Delta\bar{\phi} \propto |U_D - U_D^*|^{1/2}$, $\Delta\bar{\chi} \propto |U_S - U_S^*|^{1/2}$.

While for the case with $u_{\phi\chi}^2 - u_\phi u_\chi < 0$, there exists an intermediate phase that assumes both the non-zero SDW and the non-zero CDW order parameter, whose explicit

forms read

$$\chi^2 = \frac{u_{\phi\chi}r_\phi - r_\chi u_\phi}{u_{\phi\chi}^2 - u_\phi u_\chi}, \quad \phi^2 = \frac{u_{\phi\chi}r_\chi - r_\phi u_\chi}{u_{\phi\chi}^2 - u_\phi u_\chi}, \quad (\text{S-17})$$

from which one can directly show that the phase boundary of this intermediate phase regime is determined by

$$r_\phi \frac{u_{\phi\chi}}{u_\phi} \leq r_\chi \leq r_\phi \frac{u_\chi}{u_{\phi\chi}}. \quad (\text{S-18})$$

The transition from this intermediate phase to either the SDW or the CDW phase is the second-order transition. Moreover, both the homogeneous-SDW and homogeneous-CDW transitions are second-order transitions. From the phase diagram of the GL effective theory, we see that all these four different second-order transition lines meet at the same point ($r_\phi = 0, r_\chi = 0$), giving rise to the tetracritical point.

* liang.he@scnu.edu.cn

† syi@itp.ac.cn

- [1] M. Landini, N. Dogra, K. Kroeger, L. Hruby, T. Donner, and T. Esslinger, Phys. Rev. Lett. **120**, 223602 (2018).
- [2] R. Landig, L. Hruby, N. Dogra, M. Landini, R. Mottl, T. Donner, and T. Esslinger, Nature (London) **532**, 476 (2016).